ANTIOXIDANTS & REDOX SIGNALING
Volume 13, Number 8, 2010

DOI: 10.1089/ars.2009.3079

ORIGINAL RESEARCH COMMUNICATION

B- to Plasma-Cell Terminal Differentiation Entails Oxidative Stress and Profound Reshaping of the Antioxidant Responses

Milena Bertolotti,[1,*] Sun Hee Yim,[2,*] Jose M. Garcia-Manteiga,[1,*] Silvia Masciarelli,[1] Yoo-Jin Kim,[2] Min-Hee Kang,[2] Yoshihito Iuchi,[3] Junichi Fujii,[3] Roberta Vené,[4] Anna Rubartelli,[4] Sue Goo Rhee,[2] and Roberto Sitia[1,5]

Abstract

Limited amounts of reactive oxygen species are necessary for cell survival and signaling, but their excess causes oxidative stress. H_2O_2 and other reactive oxygen species are formed as byproducts of several metabolic pathways, possibly including oxidative protein folding in the endoplasmic reticulum. B- to plasma-cell differentiation is characterized by a massive expansion of the endoplasmic reticulum, finalized to sustain abundant immunoglobulin (Ig) synthesis and secretion. The increased production of disulfide-rich Ig might cause oxidative stress that could serve signaling roles in the differentiation and lifespan control of antibody-secreting cells. Here we show that terminal B-cell differentiation entails redox stress, NF-E2-related factor-2 (Nrf2) activation, and reshaping of the antioxidant responses. However, plasma-cell differentiation was not dramatically impaired in peroxiredoxin (Prx)1-, 2-, 3-, and 4-, glutathione peroxidase 1-, and Nrf2-knockout splenocytes, suggesting redundancy and robustness in antioxidant systems. Endoplasmic reticulum (ER)-resident Prx4 increases dramatically during differentiation. In its absence, IgM secretion was not significantly affected, but more high-molecular-weight covalent complexes accumulated intracellularly. Our results suggest that the early intracellular production of H_2O_2 facilitates B-cell proliferation and reveal a role for the Nrf2 pathway in the differentiation and function of IgM-secreting cells. *Antioxid. Redox Signal.* 13, 1133–1144.

Introduction

Upon antigen or mitogen stimulation, B lymphocytes start a differentiation process that culminates with massive production and secretion of antibodies. Differentiation entails radical changes in the structure (development of the secretory apparatus), function (immunoglobulin [Ig] secretion), and life-span control (8). After a few days of intense secretion, plasma cells that do not home into the bone marrow undergo apoptosis, limiting antibody responses (14, 40, 46).

To sustain massive Ig secretion, plasma cells are exposed to different metabolic stresses (8, 12, 19) likely including redox disequilibria (30, 42). Redox regulation controls also the onset of IgM secretion. Naive B cells are unable to form polymers and, hence, retain and eventually degrade unpolymerized subunits via thiol-dependent mechanisms. In contrast, plasma cells acquire the ability to form and secrete IgM polymers (11, 43). Igs are rich in disulfide bonds, whose formation in the endoplasmic reticulum (ER) is catalyzed by protein disulfide isomerase (PDI) and Ero1 flavoproteins (32, 50). *In vitro*, the latter can utilize oxygen as an electron acceptor, yielding H_2O_2 in equimolar amounts to the disulfides formed (13, 49, 54). If a similar pathway is also operating in living cells, the formation of up to 10^5 disulfides per second by a single plasma cell (30, 42) could generate abundant reactive oxygen species (ROS). Besides Ero1 members, other ER-resident enzymes (e.g., cytochrome P450s, flavin-containing monooxygenases, and prolyl and lysyl hydroxylases) can generate ROS as byproducts (3). In professional secretory cells, therefore, the ER can become an important source of ROS (30).

ROS are often associated with cell-damaging events, senescence, and death. However, they also act as key messengers,

[1]Division of Genetics and Cell Biology, San Raffaele Scientific Institute, Milano, Italy.
[2]Division of Life and Pharmaceutical Sciences, Ewha Womans University, Seoul, South Korea.
[3]Department of Biochemistry, Yamagata University, School of Medicine, Yamagata, Japan.
[4]Laboratory of Cell Biology, Istituto Nazionale per la Ricerca sul Cancro, Genova, Italy.
[5]Università Vita-Salute San Raffaele, Milano, Italy.
*These authors contributed equally to this work.

causing rapid and reversible posttranslational modifications, similar to protein phosphorylation. Many findings indicate that ROS, particularly H_2O_2, are essential for cell functions (10, 20, 24, 26, 27), including B-cell receptor (BCR) signaling (38). Increased Ig production in differentiating B cells could generate ROS that act as signaling devices, first by promoting proliferation and architectural rearrangements and later on to cause oxidative stress and cytotoxicity (30). This signal/stress dichotomy is reminiscent of nitric oxide and offers a new view on the potential roles of peroxide. Although the presence of nitric oxide synthases has not yet been demonstrated in the ER, reactive nitrogen species (RNS) could also be formed in this organelle, because nitrosylated PDI was found to accumulate in brains manifesting neurodegenerative diseases (51).

Under physiologic conditions, excess ROS accumulation is prevented by enzymatic and nonenzymatic mechanisms that can either scavenge ROS or prevent their formation. Enzymatic antioxidant defenses include glutathione peroxidases (GPx), the thioredoxin–thioredoxin reductase system, peroxiredoxins (Prx), glutaredoxins, superoxide dismutases (SOD), and catalases. Six Prx have been identified in mammalian cells, differing in their subcellular localization and recycling mechanisms. Prx1, 2, and 6 are localized in the cytosol, Prx3 is mitochondrial, whereas Prx4 is an ER-resident protein (17). Glutathione (GSSG/GSH), nicotinamide adenine dinucleotide (NAD/NADH), nicotinamide adenine dinucleotide phosphate (NADP/NADPH), and certain vitamins also provide efficient buffers against redox alterations (28). In addition, owing to the potential toxicity of ROS, cells can rapidly activate antioxidant responses aimed at restoring redox balance. NF-E2-related factor-2 (Nrf2) is a prototype transcription factor whose nuclear transport is redox regulated. Nrf2 is normally bound to Keap1 in the cytosol. Following H_2O_2-dependent oxidation, Keap1 releases Nrf2 that can reach the nucleus and bind to antioxidant response elements in the promoter of target genes, inducing their expression (25).

To shed light onto the dynamics of redox responses during B-cell differentiation, we analyzed here lipopolysaccharide (LPS)-activated B splenocytes from mice lacking one or more antioxidant enzymes. Our results reveal two waves of ROS production during B-cell differentiation, corresponding to the proliferative and secretory phases, respectively. The ER-resident Prx4 increases concomitantly with the development of the secretory phenotype. The absence of H_2O_2 scavengers enhances proliferation, whereas splenocytes lacking Nrf2 display defective IgM secretion. Altogether, our findings suggest that redox remodeling is important for orchestrating B- to plasma-cell differentiation.

Materials and Methods

Animal models

Male C57BL6J mice were obtained from Jackson Laboratory (Bar Harbor, ME) and maintained on a 12-h light, 12-h dark cycle. Breeding pairs of Nrf2-knockout ($Nrf2^{-/-}$) mice were obtained from RIKEN BioResource Center (Tsukuba, Japan), and $Nrf2^{+/+}$ littermates were used as wild-type (WT) controls. WT and Prx1, 2, and 3 knockout mice with 129/SvJ background were maintained in the pathogen-free authorized facility in the Division of Life and Pharmaceutical Sciences, Ewha Womans University. $Prx4^{-/-}$ were generated and maintained as previously described (18). For control experiments, we utilized mice from FVB/N background (Charles River, Milano, Italy). Mice were around 8–10 weeks of age and were allowed free access to food and water. All animal experiments were approved by the Animal Care and Use Committees of Ewha Womans University and San Raffaele Scientific Institute.

Cell cultures and spleen B-cell isolation

CD19+ B splenocytes were purified by magnetic isolation with anti-CD19 beads (Miltenyi Biotec, Bergisch Gladbach, Germany) and large size (LS)+ magnetic-activated cell sorting (MACS) separation columns following the manufacturer instructions and cultured in Roswell Park Memorial Institute medium (RPMI) with 10% endotoxin-free fetal calf serum (FCS; Hyclone Serum-Defined; Celbio, Milano, Italy), 100 U/mL Pen/Strep, 1 mM sodium pyruvate, 2 mM *N*-glutamine (Gibco–Invitrogen, Carlsbad, CA), and 50 μM 2-mercaptoethanol. Primary B cells were induced to differentiate by addition of 2–20 μg/mL LPS (Sigma, St. Louis, MO). Cells were never allowed to reach a cell density higher than 2×10^6 mL^{-1} to avoid risk of starvation. Cultures were diluted with complete medium without LPS. Cells from two or three spleens of mice with the same genotype, sex, and age were pooled together for each differentiation experiment. Proliferation curves were plotted by calculating the putative final cell number on the different time points of differentiation using different batch cultures for different days.

Flow cytometry

About 5×10^5 to 1×10^6 differentiating B cells were washed in phosphate-buffered saline/0.5% bovine serum albumine (BSA) and stained with each of the following reagents for the indicated time periods: 0.5 μg/mL propidium iodide (15 min), 5 mM Peroxy Green 1 (15 min; Peroxy-Green 1 was kindly provided by Dr. Chris Chang, Berkley) (33), 5 μM 2′,7′-dichlorofluorescein (H_2DCF-DA) (30 min at room temperature; Molecular Probes–Invitrogen, Eugene, OR), 1:200 phycoerythrin (PE)-conjugated anti-CD138 (30 min; BD Pharmingen, San Diego, CA), and 1:10,000 fluorescein isothiocyanate (FITC)-conjugated anti-μ (30 min; Cappell-ICN Pharmaceuticals, Costa Mesa, CA). Apoptosis was assessed by Annexin V–propidium iodide (PI) staining following the manufacturer's instructions (BD Bioscience, San Jose, CA). After extensive washing, samples were analyzed by FACSCalibur and data were analyzed by the CellQuestPRO (BD Bioscience) or FCS Express (De Novo Software, Los Angeles, CA) softwares.

Real-time polymerase chain reaction

Total RNA was isolated from cells by using Trizol (Invitrogen) following the manufacturer instructions and its quality checked by OD 260–280 readings and electrophoresis. Total RNA (0.5–1 μg) was retrotranscribed by the Super-Script II kit (Invitrogen) in a final volume of 10 μL, and 0.5–1 μL of the latter was used in each polymerase chain reaction. Real-time polymerase chain reaction was performed with Sybr Green Master Mix in a final volume of 25 μL by the ABI7900 HT thermal cycler (Applied Biosystems, Foster City, CA). Data were analyzed by the automated software SDS 2.1 (Applied Biosystems). The increase of each transcript at a given time point of differentiation relatively to day 0 was calculated by the $\Delta\Delta$Ct method using histone 3 as reference gene. The specific primers used were: forward 5′-tcagtccttgga

gttgcaca-3′ and reverse 5′-acacagcaggaggcaagatt-3′ (for glutamate cysteine ligase modifier); forward 5′-ccactgagctgg gaagagac-3′ and reverse 5′-tcatgatcgaaggacaccaa-3′ (for *GCLC*); forward 5′-acgcatatacccgctacctg-3′ and reverse 5′-aaggcggtcttagcctcttc-3′ (for heme oxygenase 1 [*HMOX1*]); forward 5′-agcaaagccaagatctccaa-3′ and reverse 5′-ttcaattcg atccccaaaag-3′ (for *PRX4*); forward 5′-tgccagatggacaattcaaa-3′ and reverse 5′-ggtcccaatcctccttgttt-3′ (for *PRX1*); forward 5′-tggacaccagagtcccctac-3′ and reverse 5′-tcaaggcattggaaggattc-3′ (for *PRX3*); forward 5′-agtccaccgtgtatgccttc-3′ and reverse 5′-tctgcagatcgttcatctcg-3′ (for *GPX1*); forward 5′-tcaccattgtgg caagtgtt-3′ and reverse 5′-gtgcccacagagcctagaag-3′ (for *SRX1*).

Western blotting

Total cell extracts were prepared by lysis in a buffer containing 25 mM Tris, 100 mM NaCl, 3 mM ethylenediaminetetraacetic acid, 2% sodium dodecyl sulfate (SDS) plus freshly added protease inhibitors (Roche, Basel, CH), and 10 mM N-Ethylmaleimide (NEM) (Sigma), followed by sonication to fragment DNA and heating for 10–15 min at 95°C. Postnuclear supernatants were prepared by lysing cells in 10 mM Tris HCl (pH 7.4), 150 mM NaCl, 1% NP40 plus freshly added protease inhibitors, and 10 mM NEM. Nuclear extracts were prepared by resuspending nuclear pellets in 25 mM Tris, 100 mM NaCl, 3 mM ethylenediaminetetraacetic acid, 2% SDS plus protease inhibitors, and 10 mM NEM.

To detect IgM assembly intermediates, total cell lysates were separated on polyacrylamide gradient gels (4%–14%). Stacking gels were also blotted to visualize high-molecular-weight (HMW) IgM aggregates that do not enter the resolving gel (29). To detect other proteins, conventional SDS–polyacrylamide gel electrophoresis was performed.

Polyclonal anti-Prx 1–6 antibodies were purchased from AB Frontier (Seoul, South Korea), anti-μ from Zymed (South San Francisco, CA), anti-H3 histone from Abcam (Cambridge, MA), and monoclonal antiactin from Sigma. Western blot (WB) images were acquired with the Chemidoc-it Imaging System (UVP, Upland, CA) and processed with Adobe Photoshop 7.0 (Adobe Systems, Inc., San Jose, CA). Densitometric analyses were performed using the Image Quant 5.2 software (Molecular Dynamic, Sunnyvale, CA).

Secretion assays and enzyme-linked immunosorbent assay

Differentiating B cells were washed twice in phosphate-buffered saline and cultured in Hybridoma–SFM or OptiMem Medium (Gibco) in the absence of FCS for 4 h at a cell density of 1×10^6 mL^{-1}. After centrifugation, spent media were supplemented with protease inhibitors and 10 mM NEM and analyzed by Western blotting or enzyme-linked immunosorbent assay. Aliquots of suitably diluted samples were added to anti-μ–coated plates and incubated overnight at 4°C. After extensive washes, anti-μ-HRP 1:1000 (Southern Biotechnology, Birmingham, AL) was added and incubated for 1 h at room temperature. The assay was developed with Sigma OPD fast read or tetramethylbenzidine (Invitrogen) and the plates were read at 450 nm.

Statistical analyses

Data are expressed as mean ± standard error of the mean (SEM) or standard deviation (SD), as indicated. Two-tailed Student's *t*-tests were used for comparing different samples, and significant differences were defined by *p*-values of <0.05 (*), <0.01 (**), or more (***), unless otherwise stated.

Results

Production of H_2O_2 and proliferation during B-cell differentiation in WT and Prx-deficient mice

To determine whether the transition from B lymphocytes to antibody-secreting plasma cells entails redox stress, we monitored H_2O_2 production, staining LPS-activated splenocytes with Peroxy Green 1, whose caged fluorophore is activated specifically by H_2O_2 (33). Intracellular H_2O_2 levels changed significantly during B-cell differentiation, increasing sharply in the first days after LPS activation (Fig. 1A) and rising again at the end of the culture period, before massive apoptosis ensues. The H_2O_2 increase was more marked in larger differentiated cells than in smaller ones (Supplemental Fig. 1; *see* www.liebertonline.com/ars). Although this biphasic increase was evident in most experiments, the intensity

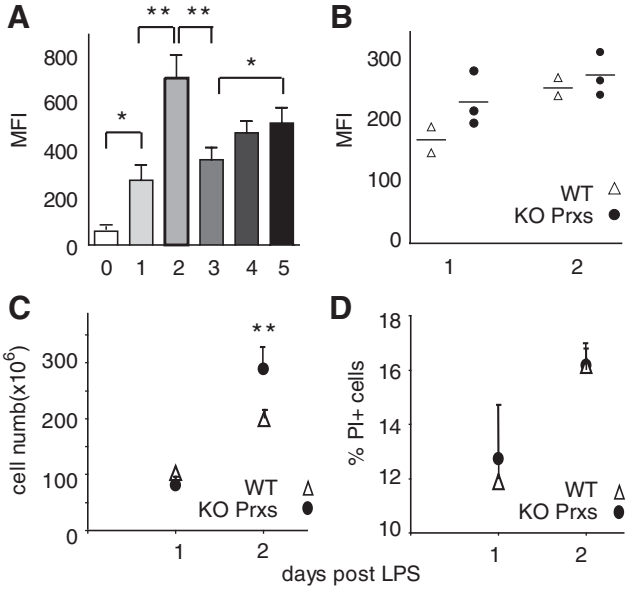

FIG. 1. H_2O_2 production and proliferation in differentiating B splenocytes. (**A**) CD19$^+$ B cells were isolated from C57BL/6J mice, stimulated with LPS *in vitro*, stained with Peroxy Green 1 to detect intracellular H_2O_2, and analyzed by flow cytometry. Data are expressed as median fluorescence intensity (MFI) in living cells ± SD (mean of seven independent experiments). *$p<0.05$, **$p<0.01$. (**B**) H_2O_2 levels in activated B splenocytes from wild-type (WT) (129/SVJ× C57BL/6 background) and peroxiredoxins (Prx)-knockout mice (each symbol represents a sample from WT [*white triangles*] or the three different knockout mice, Prx1$^{-/-}$, Prx2$^{-/-}$, and Prx3$^{-/-}$ [*black circles*]) at 24 and 48 h after LPS stimulation. The different H_2O_2 levels in WT with respect to **A** likely reflect strain differences. $p>0.05$. (**C**, **D**) Cell proliferation and cell death after LPS induction were determined as described in Materials and Methods, taking the number of B cells isolated from three spleens as starting point. Average of three mice ± SEM. **$p<0.01$. In **D**, there is no statistically significant difference between WT and KO splenocytes; the *p*-values by *t*-test are 0.51 for day 1 and 0.37 for day 2, respectively.

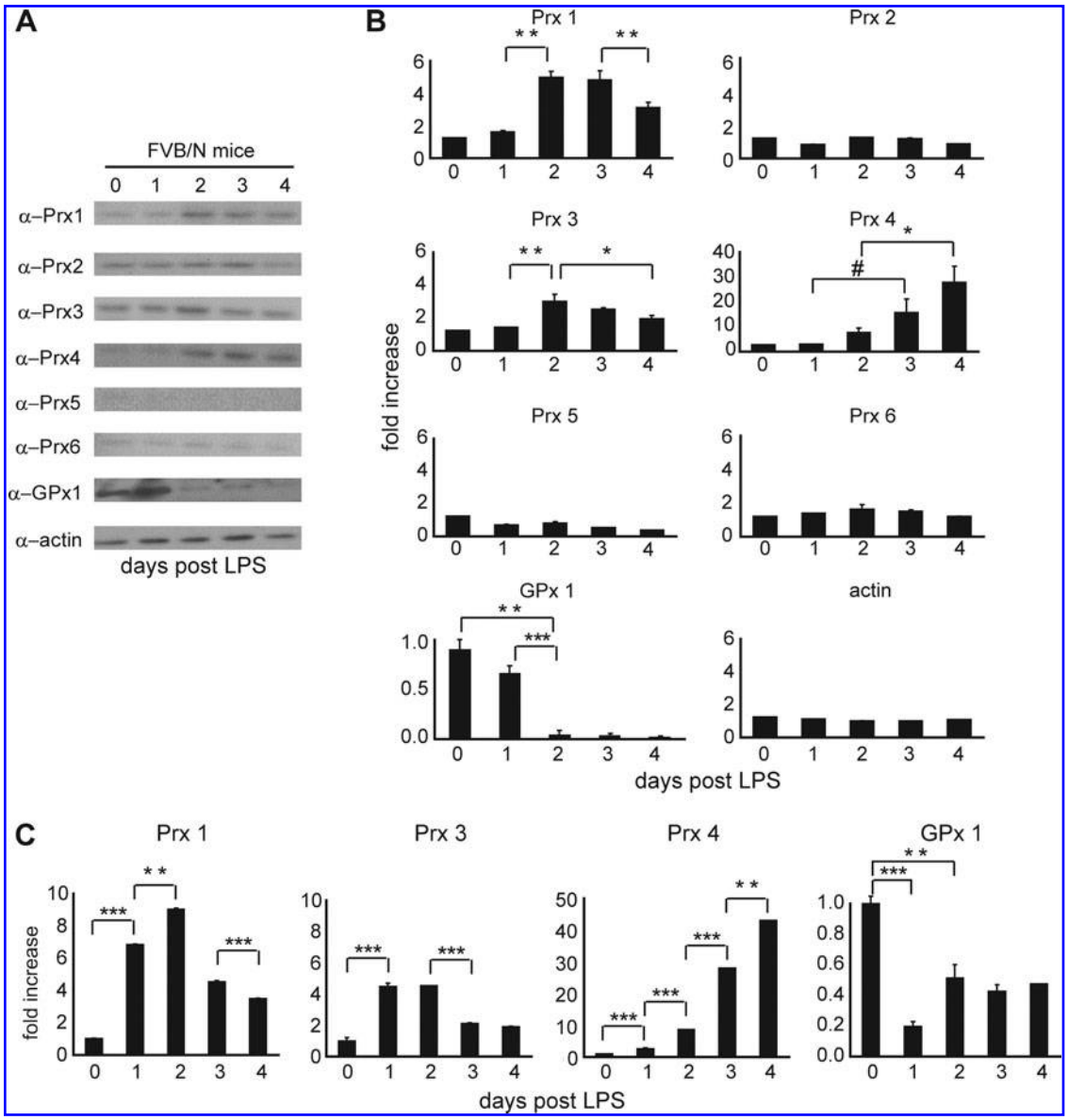

FIG. 2. Reshaping of antioxidant responses in LPS-treated mouse B splenocytes. (**A**) The panel shows a representative immunoblot of antioxidant proteins in differentiating B cells from FVB/N mice. Actin served as a loading control. (**B**) Densitometric quantification of the mean of four independent experiments similar to the one shown in **A**. $^{*}p < 0.05$, $^{**}p < 0.01$, $^{***}p < 0.001$, $^{\#}p < 0.06$. (**C**) *Prx1*, *Prx3*, *Prx4*, and glutathione peroxidase 1 (*GPx1*) transcripts were evaluated by real-time polymerase chain reaction (PCR). Histone H3 was used as a control. The results, relative to two independent experiments (FVB/N mice), are expressed as fold increase after normalization against *H3* and relative to the untreated sample. The average of three samples ± SEM was used. $^{**}p < 0.01$, $^{***}p < 0.001$.

and timing of the peaks varied significantly from strain to strain and to a minor extent also within single experiments. Similar results were obtained with 2′,7′-dichlorofluorescein (DCF), which reacts with H_2O_2 and other ROS (53). Taken together, these results indicate that B-cell differentiation entails accumulation of intracellular ROS, particularly H_2O_2.

Higher proliferative rates in B cells lacking antioxidant enzymes

ROS signaling is of prime importance for cell physiopathology and host defenses (34). H_2O_2 is an important second messenger in BCR activation (38), as for other tyrosine kinase receptors (48, 55). To determine whether the H_2O_2 rise observed in the first phase of B-cell differentiation could contribute to proliferation, we analyzed splenocytes from mice lacking Prx1, 2, or 3. More $Prx^{-/-}$ than WT cells accumulated after 2 days of culture with LPS (Fig. 1C). Cell death patterns were similar (Fig. 1D), suggesting higher proliferation rates in $Prx^{-/-}$ cells. Consistent with a proliferative role of H_2O_2 in the early phases of B-cell differentiation (22), slightly higher H_2O_2 levels were observed in the knockout mice in the first 2 days after LPS stimulation, when B cells undergo proliferation (Fig. 1B).

Next, we quantified the protein and mRNA levels of enzymes that protect cells against oxidative stress. Amongst

these, Prx scavenge hydrogen peroxide, peroxynitrite, and a wide range of organic hydroperoxides (ROOH) (39). As detected by Western blots (Fig. 2A, B), Prx1, 3, and 4 levels increased during B-cell differentiation, although with different temporal expression patterns. Prx1 and 3 peaked at days 2 and 3 and decreased thereafter, whereas Prx4 sharply increased especially in the last days of culture (note the different scale bar in Fig. 2B). A similar pattern was observed when the corresponding transcripts were analyzed (Fig. 2C). In contrast, GPx1 (15) rapidly decreased after B cells were exposed to LPS (Fig. 2A–C). Thus, Prx1 and 3 could counteract the rise in H_2O_2 levels in the first days of differentiation, despite the decrease in GPx1. The subsequent relative reduction of the cytosolic and mitochondrial buffering capacity and the increase in Prx4 parallel the development of the necessary ER and onset of IgM secretion (29, 52).

Activation of Nrf2-dependent responses during B-cell differentiation

Following H_2O_2-dependent Keap1 oxidation, Nrf2 is released and can migrate to the nucleus where it activates the transcription of genes with antioxidant response element box in their promoters (25). Consistent with the sharp increase in H_2O_2 (Fig. 1A), LPS induced nuclear accumulation of Nrf2 (Fig. 3A, B). Total Nrf2 levels increased as well in the first 2 days of differentiation, corresponding to the proliferative phase. This pattern correlated with the activation of two Nrf2-dependent genes, that is, glutamate cysteine ligase modifier involved in GSH biosynthesis and HMOX1. These results confirmed that the Nrf2 pathway is activated early upon LPS stimulation (Fig. 3C).

Terminal B-lymphocyte differentiation in mice lacking Prx3 or 4

To investigate more deeply the antioxidant network activated during B- to plasma-cell differentiation, we first compared Nrf2 activation in WT and Prx3$^{-/-}$ cells (Fig. 4A, B). Consistent with an H_2O_2-scavenging role of Prx3 in the mitochondria, cells lacking this enzyme had higher basal levels of Nrf2. However, Nrf2 increased less sharply upon LPS challenge. This correlated with less-efficient IgM secretion, as revealed by immunoblotting (Fig. 4C) or enzyme-linked immunosorbent assay (Fig. 4D) and delayed CD138 expression in Prx3$^{-/-}$ cells (Fig. 4E).

In view of the sharp increase of Prx4 during terminal B-cell differentiation (Fig. 2A–C), we analyzed splenocytes lacking this ER-resident scavenger (Fig. 5). Surprisingly, as assessed by DCF staining, we could not detect significant differences in the ROS levels between WT and Prx4$^{-/-}$ cells (Fig. 5A), and plasma-cell differentiation proceeded rather normally, as judged by monitoring proliferation, CD138 expression, and apoptosis (Fig. 5B–D). Prx4$^{-/-}$ ASC accumulated more intracellular μ chains (Fig. 5F), even though IgM secretion was not significantly impaired (Fig. 5E). HMW IgM polymers were more abundant in Prx4$^{-/-}$ ASC (Fig. 5G). Panel H shows a gel that was overrun on purpose, to better document the accumulation of HMW complexes in Prx4$^{-/-}$ splenocytes. Similar covalent complexes can be induced by exposing cells to diamide (J.M. Garcia-Manteiga and R. Sitia, unpublished results). Taken together, these results suggest that the process of IgM polymerization and quality control are

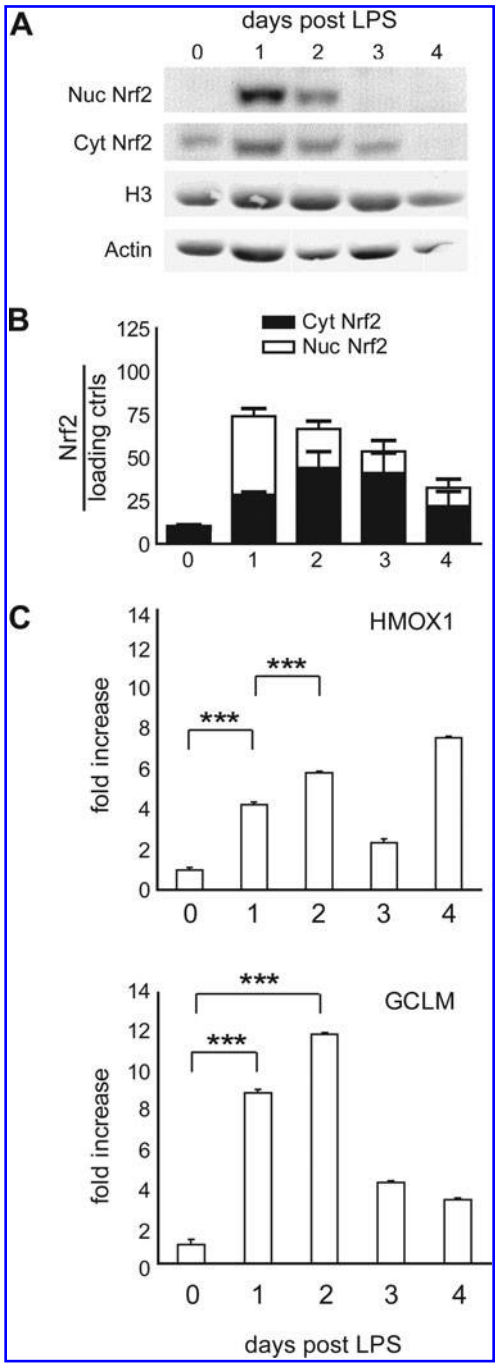

FIG. 3. Activation of NF-E2-related factor-2 (Nrf2)-dependent responses during B-cell differentiation. (**A**) Immunoblot of Nrf2 protein in nuclear and cytoplasmic extracts of B splenocytes treated with LPS for the indicated times. Actin and histone H3 were used as cytoplasmic and nuclear loading controls, respectively. (**B**) Densitometric quantification of the mean of three independent experiments similar to the one shown in **A**. Each bar indicates total cellular Nrf2, divided into nuclear and cytosolic Nrf2 (white and black sections, respectively). (**C**) Heme oxygenase 1 (*HMOX1*) and glutamate cysteine ligase modifier (*GCLM*) mRNAs were evaluated by real-time PCR. Histone H3 served as a control. The results are expressed as fold increase after normalization against *H3* and relative to the untreated sample. Bars represent means of two independent experiments ± SD (FVB/N background mice). ***$p < 0.001$.

impaired in the absence of Prx4. Although enough native polymers are secreted, more transport-incompetent, disulfide-linked HMW complexes are formed and/or inefficiently reduced, leading to intracellular accumulation. This seems to cause ER stress, as more ER-resident chaperones accumulate in Prx4$^{-/-}$ cells (Fig. 5I). In addition, higher levels of Trx1, Trx2, Prx1, and Prx2 were present in Prx4$^{-/-}$ ASC, suggesting activation of compensatory responses (Fig. 5I).

Impaired IgM secretion by plasma cells lacking Nrf2

Having shown that Nrf2-dependent responses are activated early during B-cell differentiation, we next investigated the consequences of interrupting this pathway. As expected, the Nrf2-regulated genes *GCLC*, *HMOX1*, and *SRX1* (1, 2, 9) were not induced in LPS-stimulated Nrf2$^{-/-}$ B cells (Fig. 6A). Interestingly, in the last days of differentiation, *HMOX1* transcripts became slightly more abundant also in Nrf2$^{-/-}$ splenocytes. This result may be related to our previous observation that *HMOX1* transcripts increase in day-4 WT ASC when Nrf2 is barely detectable in the nucleus and *GCLC* is no longer transcribed (Fig. 3) and it suggests alternative, Nrf2-independent pathways for *HMOX1* activation. In contrast, the expression patterns of other antioxidant factors were similar in Nrf2$^{-/-}$ splenocytes, except for a slightly lower increase in Prx1 protein levels at days 3 and 4, a slightly delayed induction of thioredoxin (Trx), a key regulator of redox homeostasis and Prx catalytic cycle (39), and of calreticulin (Crt), an ER-resident lectin chaperone (Fig. 6B, C). The basal levels of GPx1 and catalase (a peroxisomal hydrogen peroxide detoxifier) were lower in Nrf2$^{-/-}$ than in control B splenocytes. Catalase was also downregulated in differentiating B cells, albeit at a lower level than GPx1 (Fig. 6B, C).

Nrf2$^{-/-}$ cells showed similar proliferation rates with respect to WT littermates (Fig. 7A). The onset of cell death was slightly delayed (Fig. 7B) and CD138 expression reached lower levels compared with WT (Fig. 7C; see also Supplemental Fig. 2; *see* www.liebertonline.com/ars). Nrf2$^{-/-}$ cells also tended to accumulate slightly less H_2O_2 (Fig. 7D), an unexpected result in view of the lower induction of Prx1 and other H_2O_2-detoxifying enzymes in cells lacking the transcription factor. Although the above differences were rather subtle, a clear difference was evident with respect to IgM secretion (panels E–G). Differentiating Nrf2$^{-/-}$ cells secreted less IgM (panels E and G). The reduction in IgG secretion was less marked (Fig. 7G, lower panel). Nrf2$^{-/-}$ cells accumulated slightly less intracellular Ig-μ chains (panel F), intracellular polymers being selectively underrepresented (panel E). This pattern differs significantly to the one observed in Prx4$^{-/-}$ splenocytes, where normal secretion was accompanied by increased intracellular accumulation. In contrast, the reduced IgM secretion observed in Nrf2$^{-/-}$ splenocytes is reminiscent of the phenotype of Prx3$^{-/-}$ ASC, in which Nrf2 levels were lower (Fig. 4).

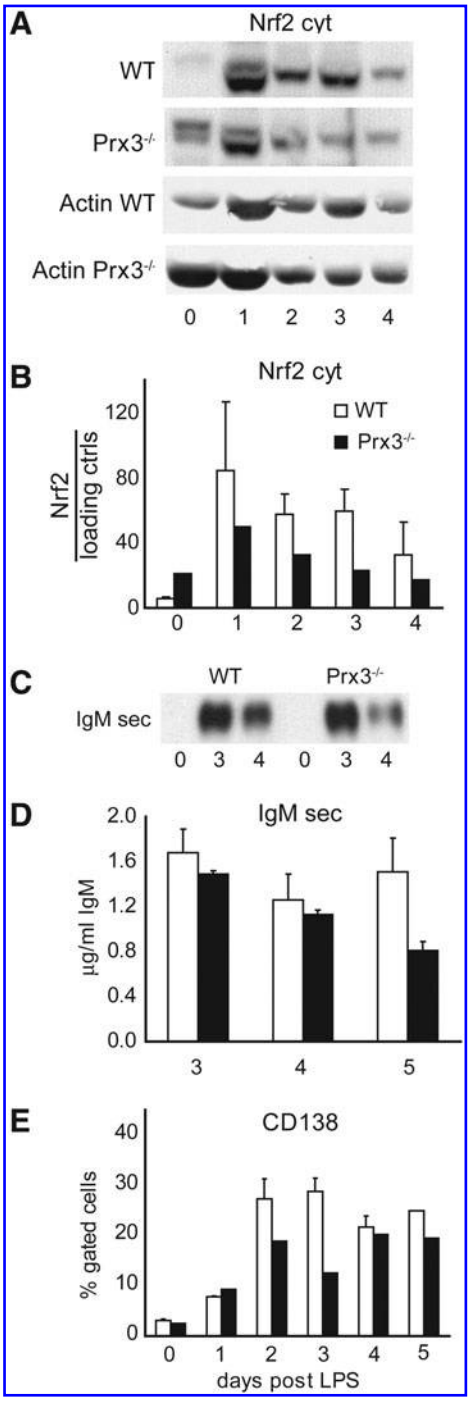

FIG. 4. Analysis of Prx3$^{-/-}$ LPS-stimulated splenocytes. (**A**) Immunoblot of Nrf2 protein in cytoplasmic extracts of B splenocytes from WT and Prx3$^{-/-}$ mice treated with LPS for the indicated times. Actin was used as a loading control. The two bands observed here are consistent with the binding pattern observed for other commercially available antibodies to Nrf2; the heaviest one may correspond to ubiquitinated Nrf2. (**B**) Densitometric quantification of cytosolic Nrf2 band in cytoplasmic extracts of the experiment shown in **A**. Bars represent triplicates from a single experiment ± SD. (**C**, **D**) IgM secretion was monitored by analyzing aliquots of the spent media collected after 4 h of culture (10^6 cells/mL) in fresh medium by immunoblotting with anti-μ (**C**), or by enzyme-linked immunosorbent assay (ELISA) (**D**). Bars represent the means of two experiments ± SD. The differences were not statistically significant (p-values = 0.4, 0.6, and 0.1 at days 3, 4, and 5, respectively). (**E**) Surface expression of CD138/syndecan-1 was monitored by fluorescence-activated cell sorting (FACS) analyses. Bars represent duplicates from one experiment ± SD (two different sets of samples were used for WT littermates of the same strain).

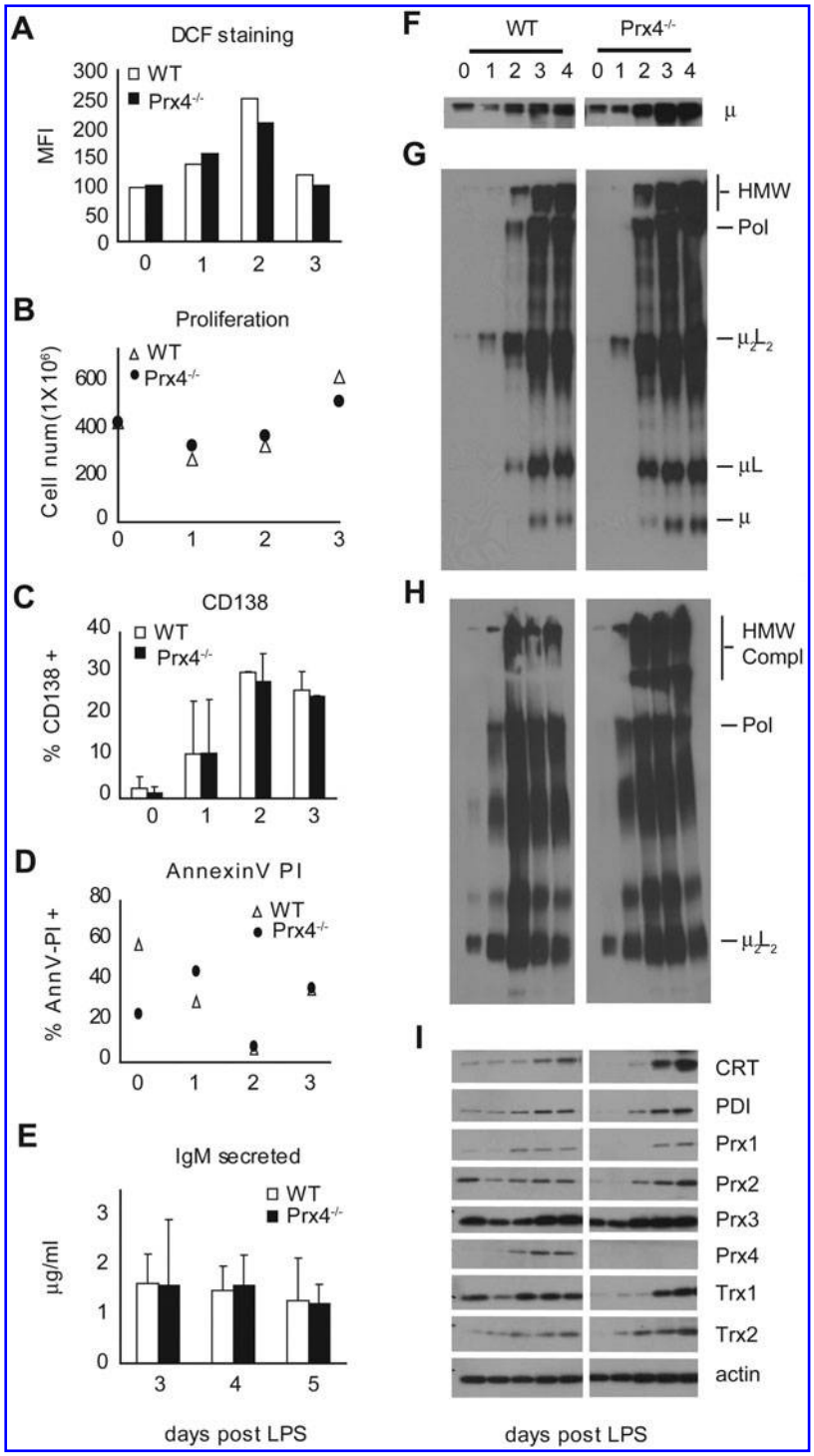

FIG. 5. B-cell differentiation in Prx4$^{-/-}$ cells. (**A**) DCF staining for reactive oxygen species in WT and Prx4$^{-/-}$ B lymphocytes at different times upon exposure to LPS. Data are expressed as MFI in living cells. (**B**–**D**) B-cell differentiation was followed by monitoring proliferation (**B**), CD138 expression (**C**), and apoptosis (**D**), as described in the Materials and Methods section. Bars represent means of two independent sets of samples ± SD. (**E**) Secretion efficiency of WT and Prx4$^{-/-}$ ASC at 3, 4, and 5 days after LPS stimulation was tested by ELISA of the spent media after 4 h of culture (10^6 cells/mL) in fresh medium (SD was calculated for two independent sets of samples). (**F**–**H**) Accumulation of high-molecular-weight (HWM) IgM complexes in Prx4$^{-/-}$ cells. Aliquots from the cell lysates were resolved under reducing (**F**) or nonreducing (**G**, **H**) conditions. The nitrocellulose filters were decorated with anti-μ chain antibodies. The gel shown in **H** was polymerized and run to increase the resolution of HWM species. The main IgM assembly intermediates are indicated on the right-hand margin. (**I**) Expression of antioxidants and ER-resident proteins in WT and Prx4$^{-/-}$ splenocytes was evaluated by immunoblotting with specific antibodies, as described in the legend of Figure 2. The panel shows representative gels out of two independent experiments.

Discussion

Terminal B-lymphocyte differentiation provides a powerful system to dissect how dramatic changes in cell architecture, protein synthesis, secretion, and life-span control are integrated (30). We show here that partially redundant redox responses are activated and contribute to orchestrate plasma-cell differentiation.

Upon *ex vivo* LPS stimulation, B lymphocytes experience oxidative stress, as shown by increased H_2O_2 production and profound reshaping of the antioxidant responses. Prx1 and 3 follow the pattern of other cytosolic and mitochondrial proteins (52). Prx4 parallels the dramatic expansion of the ER (52), however, increasing more sharply than PDI and calreticulin (CRT). GPx1 instead rapidly decreases. Thus, the changes observed reflect more than the simple architectural metamorphosis that hallmarks B- to plasma-cell differentiation. It will be of interest to unveil the regulatory elements controlling the transcription of these enzymes, as some of which can become targets for altering Ig production and plasma-cell

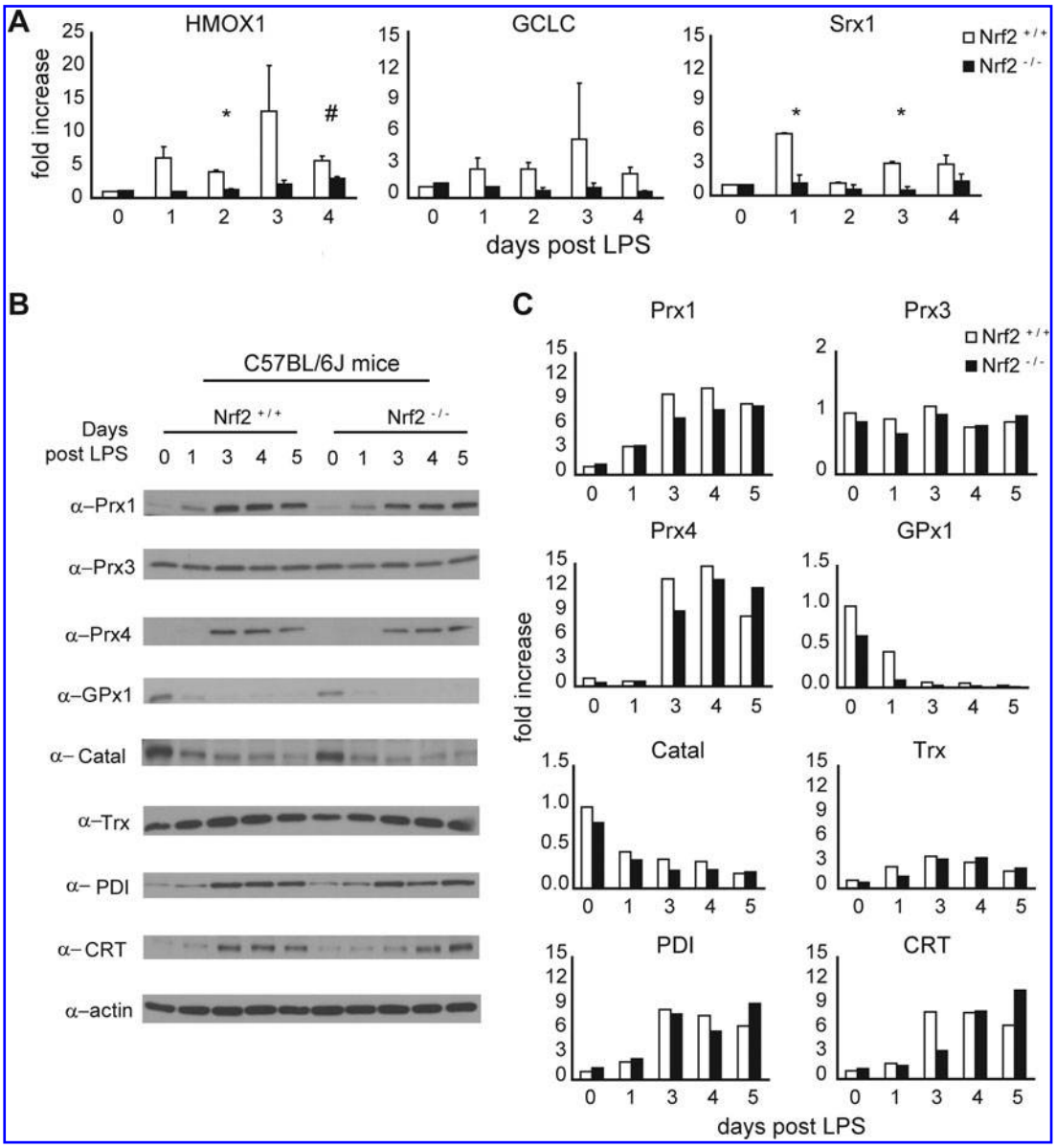

FIG. 6. Altered antioxidant responses in differentiating B cells lacking Nrf2. (**A**) Real-time PCR was used to quantify the expression of the Nrf2-regulated genes *GCLC*, *HMOX1*, and *SRX* in WT and Nrf2$^{-/-}$ differentiating B cells (C57BL/6J background). The results are expressed as fold increase after normalization against H3 and relative to the untreated sample. Bars represent means of two independent experiments ± SD. $^{*}p < 0.03$, $^{\#}p < 0.06$. (**B**, **C**) Immunoblot and densitometric quantification of redox-involved proteins in WT and Nrf2$^{-/-}$ B cells.

lifespan, a potentially important endeavor in amyloidosis and multiple myeloma (8, 44).

The initial rise in H_2O_2 correlates with proliferation, which is more rapid in B cells lacking Prx1 or Prx3 (Fig. 1C). This adds fuel to the notion that BCR signaling is promoted by the concomitant production of H_2O_2 (38). However, despite their lower H_2O_2 content during the initial phase, Nrf2$^{-/-}$ cells proliferate similarly, suggesting the involvement of additional regulatory pathways. In our experiments, LPS stimulation proceeds independently from BCR activation. However, TLR4 stimulation generates ROS in cells involved in innate immunity (31). As H_2O_2 can activate BCR signaling also in the absence of antigen (38), it is possible that its initial rise plays an important role in TLR4-dependent B-cell activation. In support of this hypothesis, GPx1, an antioxidant enzyme abundant in resting B cells, decreases sharply after LPS stimulation (Fig. 2A, B). Catalase, another ROS-scavenging enzyme shown to negatively affect cell-cycle progression in endothelial cells (36), also decreases (Fig. 6B, C). The high initial levels of GPx1 and catalase could account for a rapid ROS scavenging during the first hours after activation; indeed, only a marginal increase in ROS levels was detected before 24 h of activation (53). H_2O_2 production during the first days of differentiation parallels the induction of Prx1 and Prx3 (localized in the cytosol and the mitochondria, respectively). The initial reshaping of the antioxidant defense could help sustain the signaling role of H_2O_2; the downregulation of GPx1 and catalase could be balanced by the induction of Prx1

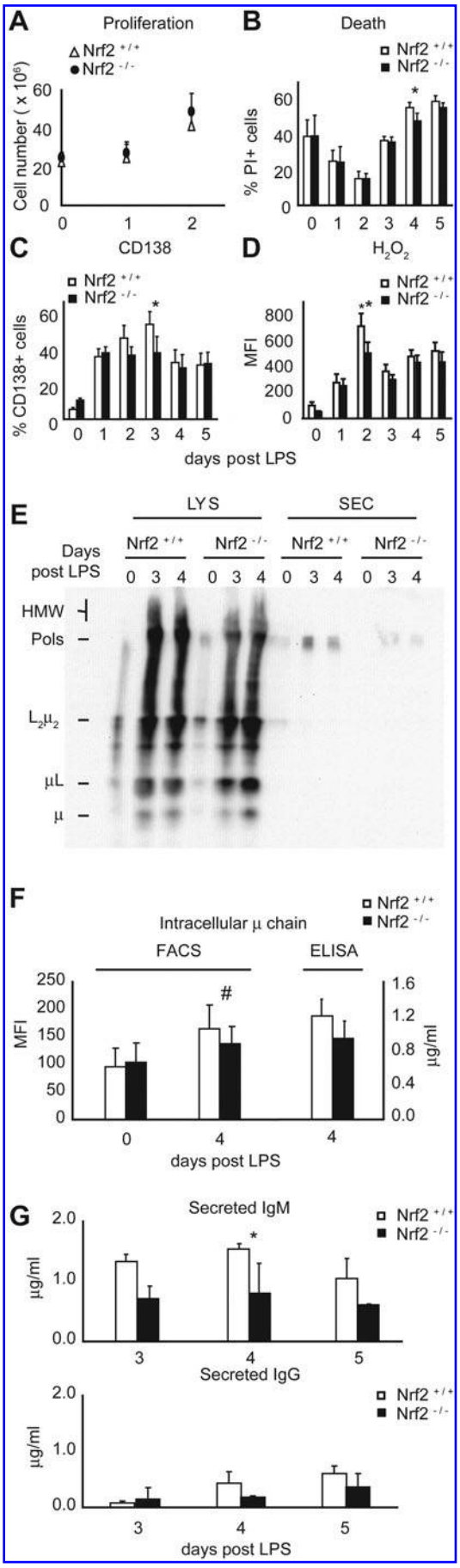

and Prx3 to prevent H_2O_2 toxicity or to modulate the duration of the proliferative signal, as the peak in their induction coincides with the end of the proliferation phase (Fig. 2B). The first wave of ROS is most probably of mitochondrial origin (53), where Prx3 is located; splenocytes from Prx3 null mice proliferated more and accumulated more H_2O_2 (Fig. 1B, C).

A key cellular defense against oxidative or electrophilic stress is the activation of Nrf2, whose pathway controls the expression of genes involved in the detoxification and elimination of reactive oxidants (35). Not surprisingly, therefore, Nrf2 translocates to the nucleus in LPS-stimulated splenocytes and HMOX1 and GLCM transcripts are increased (Fig. 3A–C).

Having shown the activation and reshaping of several antioxidant mechanisms, we analyzed their physiological relevance using splenocytes from knockout (KO) animals. In the absence of Prx3, the basal levels of Nrf2 are higher, likely reflecting reduced mitochondrial H_2O_2 scavenging. After LPS stimulation, however, Nrf2 increases less in Prx3$^{-/-}$ cells to fight against a compromised redox environment. This fact, with the unexpected observation that deletion of Prx4 has rather minor consequences on plasma-cell differentiation, suggests redundancy in the antioxidant systems and may explain why other oxidative stress indicators were not significantly affected. A corollary of these observations is that either additional scavenging systems exist in the secretory compartment, or ROS can be scavenged across compartments. Ruddock and coworkers recently proposed that H_2O_2 can sustain native disulfide formation using bovine pancreatic trypsin inhibitor (BTPI) as a model substrate (22). The abundant HMW covalent

FIG. 7. Lack of Nrf2 slightly delays plasma-cell differentiation and impairs IgM secretion. B splenocytes isolated from WT and Nrf2$^{-/-}$ spleens (C57BL/6J background) were incubated in the presence of LPS, and plasma-cell differentiation and IgM production and secretion were monitored following different parameters. (**A**) Cell proliferation was determined as described in the Materials and Methods section, taking the number of B cells isolated from one spleen as starting point. There is no statistically significant difference between WT and KO; *p*-values are 0.95 and 0.73 for days 1 and 2, respectively. (**B**) Cell death was monitored by counting PI-positive cells. $^{*}p < 0.03$. (**C**) Surface expression of CD138/syndecan-1 was monitored by FACS. $^{*}p < 0.03$. (**D**) Peroxy Green 1 staining for H_2O_2 in WT and Nrf2$^{-/-}$ B lymphocytes at different times upon exposure to LPS. Data are expressed as MFI in living cells ± SEM. All data represent the mean of seven independent samples. $^{**}p < 0.01$. (**E**) To analyze IgM polymerization, total protein extracts (LYS) and 4-h spent media (SEC) from WT and Nrf2$^{-/-}$ B cells (C57BL/6J background) were subjected to sodium dodecyl sulfate–polyacrylamide gel electrophoresis in nonreducing conditions. The nitrocellulose filter was decorated with anti-μ antibodies. The main IgM assembly intermediates are indicated on the left-hand margin. (**F**) Intracellular Ig-μ chain content was assessed by flow cytometry after staining cells with FITC-conjugated anti-μ (FACS, $n = 7$) or by ELISA ($n = 3$) for IgM on total cell lysates; values are average ± SEM. $^{\#}p < 0.07$. (**G**) Secretion efficiency of WT and Nrf2$^{-/-}$ ASC at 3, 4, and 5 days after LPS stimulation was tested by ELISA measurements of IgM and IgG concentrations after 4 h of culture (10^6 cells/mL) in fresh medium; values are average of seven experiments ± SEM. $^{*}p < 0.03$.

IgM polymers observed in Prx4$^{-/-}$ cells could reflect H_2O_2 scavenging by abundant substrate proteins. Accumulation of transport-incompetent aberrant IgM correlates with higher ER chaperone content, suggesting ER stress conditions. However, the price paid by plasma cells [intrinsically short-lived and constitutively stressed elements (8)] is low, considering that IgM secretion is essentially normal. Therefore, it is not surprising that Prx4$^{-/-}$ mice do not display an overt immunological phenotype. Moreover, it is possible that members of the GPx family reside in the ER, which could compensate for the absence of Prx4. To be effective, cross-compartmental scavenging would require rapid H_2O_2 diffusion across membranes, which contrasts with experimental data obtained in yeast (5). A better understanding of H_2O_2 transport is required to address these important issues (38).

GCLC, *HMOX1*, and *Srx1* (2, 37, 41) were not activated in Nrf2$^{-/-}$ splenocytes, confirming the involvement and relevance of the pathway (Fig. 5A). Some *HMOX1* was expressed at day 4, implying the existence of Nrf2-independent activation pathway(s). The delayed induction of Trx and calreticulin could be related to the observation that in mouse liver cells these two proteins are induced by sulforaphane in an Nrf2-dependent manner (16). As Trx plays a role in the Prx catalytic cycle (39), its delayed appearance might also reflect the lower expression of Prx1 in Nrf2$^{-/-}$ cells.

Although proliferation was not significantly affected, the expression of CD138, a marker of plasma-cell differentiation, and the onset of apoptosis were slightly delayed in Nrf2$^{-/-}$ cells (Fig. 7A–C), suggesting impaired ASC differentiation. Indeed, Nrf2$^{-/-}$ cells secreted fewer IgM molecules (Fig. 7E–G) and the overall lifespan of ASC was shown to be related to the load of protein production and secretion (4, 6, 7). Surprisingly, the lack of Nrf2 translated into lower intracellular H_2O_2 levels both in basal conditions and upon LPS activation, indicating either the activation of compensatory mechanisms, or that H_2O_2-production pathway(s) exist, which are at least in part dependent on Nrf2. LPS is known to increase the transcription of SOD (45), an H_2O_2-producing enzyme; we also detected higher expression of the protein early after LPS stimulation (data not shown). Mitochondrial SOD2 is thought to be regulated by Nrf2 (47), and Juarez *et al.* reported decreased H_2O_2 production and signaling in cells defective in SOD activity (21). We found lower SOD2 levels in Nrf2$^{-/-}$ cells (our unpublished results). Further, it has been shown that CD138 is upregulated in response to exogenous H_2O_2 (23), which may correlate with its lower levels in Nrf2$^{-/-}$ ASC.

The lack of protecting Nrf2-dependent antioxidant responses might be compensated by the dramatic increase in Prx4, an ER-resident enzyme that could scavenge ROS produced during the last phases of differentiation. This raises the questions of whether the flavoprotein-dependent oxidative folding in the ER is a source of H_2O_2, as demonstrated *in vitro*, and to what extent Prx4 can operate as an H_2O_2 scavenger, because Srx1 is not found in the exocytic compartment. Blocking protein synthesis has only a marginal effect on H_2O_2 accumulation (53). Experiments with organelle-specific reporters are needed to determine the origin of H_2O_2 and its diffusibility across biological membranes. One limitation of our experimental system has been so far the inability to efficiently transfect B lymphocytes without severely perturbing their differentiation properties. An effort to circumvent this obstacle is certainly worth, as it will be of great interest to precisely dissect the dynamic redox changes that underlie B-cell differentiation.

Acknowledgments

The authors thank Drs. Chris Chang, Michel Toledano, and Eelco Van Anken for providing reagents, advice, and criticisms, Claudio Fagioli and Elena Pasqualetto for expert technical help, and Raffaella Brambati and Ana Fella for patient secretarial assistance. This work was supported in part through grants from AIRC, Cariplo, Compagnia San Paolo, Ministero Università e Ricerca, Ministero Salute and Telethon (to R.S.) and from the National Research Foundation of Korea (National Honor Scientist program grant 2009-0052293 and Bio R&D program grant M10642040001-07N4204-00110 to S.G.R. and S.H.Y.).

Author Disclosure Statement

No competing financial interests exist.

References

1. Alam J, Stewart D, Touchard C, Boinapally S, Choi AM, and Cook JL. Nrf2, a Cap'n'Collar transcription factor, regulates induction of the heme oxygenase-1 gene. *J Biol Chem* 274: 26071–26078, 1999.
2. Bae SH, Woo HA, Sung SH, Lee HE, Lee SK, Kil IS, and Rhee SG. Induction of sulfiredoxin via an Nrf2-dependent pathway and hyperoxidation of peroxiredoxin III in the lungs of mice exposed to hyperoxia. *Antioxid Redox Signal* 11: 937–948, 2008.
3. Banhegyi G, Mandl J, and Csala M. Redox-based endoplasmic reticulum dysfunction in neurological diseases. *J Neurochem* 107: 20–34, 2008.
4. Bianchi G, Oliva L, Cascio P, Pengo N, Fontana F, Cerruti F, Orsi A, Pasqualetto E, Mezghrani A, Calbi V, Palladini G, Giuliani N, Anderson KC, Sitia R, and Cenci S. The proteasome load versus capacity balance determines apoptotic sensitivity of multiple myeloma cells to proteasome inhibition. *Blood* 113: 3040–3049, 2009.
5. Bienert GP, Moller AL, Kristiansen KA, Schulz A, Moller IM, Schjoerring JK, and Jahn TP. Specific aquaporins facilitate the diffusion of hydrogen peroxide across membranes. *J Biol Chem* 282: 1183–1192, 2007.
6. Cenci S, Mezghrani A, Cascio P, Bianchi G, Cerruti F, Fra A, Lelouard H, Masciarelli S, Mattioli L, Oliva L, Orsi A, Pasqualetto E, Pierre P, Ruffato E, Tagliavacca L, and Sitia R. Progressively impaired proteasomal capacity during terminal plasma cell differentiation. *Embo J* 25: 1104–1113, 2006.
7. Cenci S, Pengo N, and Sitia R. Proteotoxic stress and cell lifespan control. *Mol Cells* 26: 323–328, 2008.
8. Cenci S and Sitia R. Managing and exploiting stress in the antibody factory. *FEBS Lett* 581: 3652–3657, 2007.
9. Chan JY and Kwong M. Impaired expression of glutathione synthetic enzyme genes in mice with targeted deletion of the Nrf2 basic-leucine zipper protein. *Biochim Biophys Acta* 1517: 19–26, 2000.
10. Forman HJ, Fukuto JM, and Torres M. Redox signaling: thiol chemistry defines which reactive oxygen and nitrogen species can act as second messengers. *Am J Physiol Cell Physiol* 287: C246–C256, 2004.
11. Fra AM, Fagioli C, Finazzi D, Sitia R, and Alberini CM. Quality control of ER synthesized proteins: an exposed thiol

group as a three-way switch mediating assembly, retention and degradation. *EMBO J* 12: 4755–61, 1993.
12. Gass JN, Gunn KE, Sriburi R, and Brewer JW. Stressed-out B cells? Plasma-cell differentiation and the unfolded protein response. *Trends Immunol* 25: 17–24, 2004.
13. Gross E, Sevier CS, Heldman N, Vitu E, Bentzur M, Kaiser CA, Thorpe C, and Fass D. Generating disulfides enzymatically: reaction products and electron acceptors of the endoplasmic reticulum thiol oxidase Ero1p. *Proc Natl Acad Sci USA* 103: 299–304, 2006.
14. Hendershot LM and Sitia R. Immunoglobulin assembly and secretion. In: *Molecular Biology of B cells*, edited by Honjo T, Alt FW, and Neuberger M. San Diego, CA: Elsevier Academic Press, 2004, pp. 261–272.
15. Herbette S, Roeckel-Drevet P, and Drevet JR. Seleno-independent glutathione peroxidases. More than simple antioxidant scavengers. *FEBS J* 274: 2163–80, 2007.
16. Hu R, Xu C, Shen G, Jain MR, Khor TO, Gopalkrishnan A, Lin W, Reddy B, Chan JY, and Kong AN. Gene expression profiles induced by cancer chemopreventive isothiocyanate sulforaphane in the liver of C57BL/6J mice and C57BL/6J/Nrf2 (-/-) mice. *Cancer Lett* 243: 170–192, 2006.
17. Immenschuh S and Baumgart-Vogt E. Peroxiredoxins, oxidative stress, and cell proliferation. *Antioxid Redox Signal* 7: 768–777, 2005.
18. Iuchi Y, Okada F, Tsunoda S, Kibe N, Shirasawa N, Ikawa M, Okabe M, Ikeda Y, and Fujii J. Peroxiredoxin 4 knockout results in elevated spermatogenic cell death via oxidative stress. *Biochem J* 419: 149–158, 2009.
19. Iwakoshi NN, Lee AH, and Glimcher LH. The X-box binding protein-1 transcription factor is required for plasma cell differentiation and the unfolded protein response. *Immunol Rev* 194: 29–38, 2003.
20. Jones DP. Radical-free biology of oxidative stress. *Am J Physiol Cell Physiol* 295: C849–C868, 2008.
21. Juarez JC, Manuia M, Burnett ME, Betancourt O, Boivin B, Shaw DE, Tonks NK, Mazar AP, and Donate F. Superoxide dismutase 1 (SOD1) is essential for H2O2-mediated oxidation and inactivation of phosphatases in growth factor signaling. *Proc Natl Acad Sci USA* 105: 7147–7152, 2008.
22. Karala AR, Lappi AK, Saaranen MJ, and Ruddock LW. Efficient peroxide-mediated oxidative refolding of a protein at physiological pH and implications for oxidative folding in the endoplasmic reticulum. *Antioxid Redox Signal* 11: 963–970, 2009.
23. Kemp TJ, Causton HC, and Clerk A. Changes in gene expression induced by H(2)O(2) in cardiac myocytes. *Biochem Biophys Res Commun* 307: 416–421, 2003.
24. Kondo N, Nakamura H, Masutani H, and Yodoi J. Redox regulation of human thioredoxin network. *Antioxid Redox Signal* 8: 1881–1890, 2006.
25. Kwak MK, Wakabayashi N, Greenlaw JL, Yamamoto M, and Kensler TW. Antioxidants enhance mammalian proteasome expression through the Keap1-Nrf2 signaling pathway. *Mol Cell Biol* 23: 8786–8794, 2003.
26. Lillig CH and Holmgren A. Thioredoxin and related molecules—from biology to health and disease. *Antioxid Redox Signal* 9: 25–47, 2007.
27. Liu H, Colavitti R, Rovira II, and Finkel T. Redox-dependent transcriptional regulation. *Circ Res* 97: 967–974, 2005.
28. Malhotra JD and Kaufman RJ. Endoplasmic reticulum stress and oxidative stress: a vicious cycle or a double-edged sword? *Antioxid Redox Signal* 9: 2277–2293, 2007.
29. Masciarelli S, Fra AM, Pengo N, Bertolotti M, Cenci S, Fagioli C, Ron D, Hendershot LM, and Sitia R. CHOP-independent apoptosis and pathway-selective induction of the UPR in developing plasma cells. *Mol Immunol* 47: 1356–1365, 2010.
30. Masciarelli S and Sitia R. Building and operating an antibody factory: redox control during B to plasma cell terminal differentiation. *Biochim Biophys Acta* 1783: 578–588, 2008.
31. Matsuzawa A, Saegusa K, Noguchi T, Sadamitsu C, Nishitoh H, Nagai S, Koyasu S, Matsumoto K, Takeda K, and Ichijo H. ROS-dependent activation of the TRAF6-ASK1-p38 pathway is selectively required for TLR4-mediated innate immunity. *Nat Immunol* 6: 587–592, 2005.
32. Mezghrani A, Fassio A, Benham A, Simmen T, Braakman I, and Sitia R. Manipulation of oxidative protein folding and PDI redox state in mammalian cells. *EMBO J* 20: 6288–6296, 2001.
33. Miller EW, Tulyathan O, Isacoff EY, and Chang CJ. Molecular imaging of hydrogen peroxide produced for cell signaling. *Nat Chem Biol* 3: 263–267, 2007.
34. Nathan C and Shiloh MU. Reactive oxygen and nitrogen intermediates in the relationship between mammalian hosts and microbial pathogens. *Proc Natl Acad Sci USA* 97: 8841–8848, 2000.
35. Nguyen T, Nioi P, and Pickett CB. The Nrf2-antioxidant response element signaling pathway and its activation by oxidative stress. *J Biol Chem* 284: 13291–13295, 2009.
36. Onumah OE, Jules GE, Zhao Y, Zhou L, Yang H, and Guo Z. Overexpression of catalase delays G0/G1- to S-phase transition during cell cycle progression in mouse aortic endothelial cells. *Free Radic Biol Med* 46: 1658–1667, 2009.
37. Reichard JF, Motz GT, and Puga A. Heme oxygenase-1 induction by NRF2 requires inactivation of the transcriptional repressor BACH1. *Nucleic Acids Res* 35: 7074–7086, 2007.
38. Reth M. Hydrogen peroxide as second messenger in lymphocyte activation. *Nat Immunol* 3: 1129–1134, 2002.
39. Rhee SG, Yang KS, Kang SW, Woo HA, and Chang TS. Controlled elimination of intracellular H(2)O(2): regulation of peroxiredoxin, catalase, and glutathione peroxidase via post-translational modification. *Antioxid Redox Signal* 7: 619–626, 2005.
40. Shapiro-Shelef M and Calame K. Regulation of plasma-cell development. *Nat Rev Immunol* 5: 230–242, 2005.
41. Shenvi SV, Smith EJ, and Hagen TM. Transcriptional regulation of rat gamma-glutamate cysteine ligase catalytic subunit gene is mediated through a distal antioxidant response element. *Pharmacol Res* 60: 229–236, 2009.
42. Shimizu Y and Hendershot LM. Oxidative folding: cellular strategies for dealing with the resultant equimolar production of reactive oxygen species. *Antioxid Redox Signal* 11: 2317–2331, 2009.
43. Sitia R, Neuberger M, Alberini C, Bet P, Fra A, Valetti C, Williams G, and Milstein C. Developmental regulation of IgM secretion: the role of the carboxy-terminal cysteine. *Cell* 60: 781–790, 1990.
44. Sitia R, Palladini G, and Merlini G. Bortezomib in the treatment of AL amyloidosis: targeted therapy? *Haematologica* 92: 1302–1307, 2007.
45. Sugino N, Telleria CM, and Gibori G. Differential regulation of copper-zinc superoxide dismutase and manganese superoxide dismutase in the rat corpus luteum: induction of manganese superoxide dismutase messenger ribonucleic acid by inflammatory cytokines. *Biol Reprod* 59: 208–215, 1998.

46. Tarlinton D, Radbruch A, Hiepe F, and Dorner T. Plasma cell differentiation and survival. *Curr Opin Immunol* 20: 162–169, 2008.
47. Taylor RC, Acquaah-Mensah G, Singhal M, Malhotra D, and Biswal S. Network inference algorithms elucidate Nrf2 regulation of mouse lung oxidative stress. *PLoS Comput Biol* 4: e1000166, 2008.
48. Tonks NK. Redox redux: revisiting PTPs and the control of cell signaling. *Cell* 121: 667–670, 2005.
49. Tu BP and Weissman JS. The FAD- and O(2)-dependent reaction cycle of Ero1-mediated oxidative protein folding in the endoplasmic reticulum. *Mol Cell* 10: 983–994, 2002.
50. Tu BP and Weissman JS. Oxidative protein folding in eukaryotes: mechanisms and consequences. *J Cell Biol* 164: 341–346, 2004.
51. Uehara T, Nakamura T, Yao D, Shi ZQ, Gu Z, Ma Y, Masliah E, Nomura Y, and Lipton SA. S-nitrosylated protein-disulphide isomerase links protein misfolding to neurodegeneration. *Nature* 441: 513–517, 2006.
52. van Anken E, Romijn EP, Maggioni C, Mezghrani A, Sitia R, Braakman I, and Heck AJ. Sequential waves of functionally related proteins are expressed when B cells prepare for antibody secretion. *Immunity* 18: 243–253, 2003.
53. Vené R, Delfino L, Castellani P, Balza E, Bertolotti M, Sitia R, and Rubartelli A. Redox remodeling allows and controls B-cell activation and differentiation. *Antioxid Redox Signal* 13: 1145–1155, 2010.
54. Wang L, Li SJ, Sidhu A, Zhu L, Liang Y, Freedman RB, and Wang CC. Reconstitution of human Ero1-Lalpha/protein-disulfide isomerase oxidative folding pathway *in vitro*. Position-dependent differences in role between the a and a′ domains of protein-disulfide isomerase. *J Biol Chem* 284: 199–206, 2009.
55. Woo HA, Yim SH, Shin DH, Kang D, Yu DY, and Rhee SG. Inactivation of peroxiredoxin I by phosphorylation allows localized H(2)O(2) accumulation for cell signaling. *Cell* 140: 517–528, 2010.

Address correspondence to:
Dr. Roberto Sitia
Division of Genetics and Cell Biology
San Raffaele Scientific Institute
Via Olgettina 58
Milano 20132
Italy

E-mail: sitia.roberto@hsr.it

Date of first submission to ARS Central, December 29, 2009; date of final revised submission, May 17, 2010; date of acceptance, May 19, 2010.

Abbreviations Used

ASC = antibody secreting cell
BCR = B-cell receptor
DCF = 2′,7′-dichlorofluorescein
ER = endoplasmic reticulum
FACS = fluorescence-activated cell sorting
FCS = fetal calf serum
GCLC = glutamate cysteine ligase catalytic
GCLM = glutamate cysteine ligase modifier
GPx = glutathione peroxidases
HMOX1 = heme oxygenase 1
HMW = high molecular weight
Ig = immunoglobulin
KO = knockout
LPS = lipopolysaccharide
MFI = median fluorescence intensity
NEM = N-ethylmaleimide
Nrf2 = NF-E2-related factor-2
PDI = protein disulfide isomerase
PG1 = Peroxy Green 1
Prx = peroxiredoxins
ROS = reactive oxygen species
SDS = sodium dodecyl sulfate
SOD = superoxide dismutases

This article has been cited by:

1. Dr. Ester Zito . PRDX4, an ER-localised peroxiredoxin at the crossroads between enzymatic oxidative protein folding and non-enzymatic protein oxidation. *Antioxidants & Redox Signaling* **0**:ja. . [Abstract] [Full Text PDF] [Full Text PDF with Links]
2. Yuhui Yang, Svetlana Karakhanova, Sabine Soltek, Jens Werner, Pavel P. Philippov, Alexandr V. Bazhin. 2012. In vivo immunoregulatory properties of the novel mitochondria-targeted antioxidant SkQ1. *Molecular Immunology* **52**:1, 19-29. [CrossRef]
3. Éva Margittai , Péter Löw , Ibolya Stiller , Alessandra Greco , Jose Manuel Garcia-Manteiga , Niccolo Pengo , Angelo Benedetti , Roberto Sitia , Gábor Bánhegyi . 2012. Production of H2O2 in the Endoplasmic Reticulum Promotes In Vivo Disulfide Bond Formation. *Antioxidants & Redox Signaling* **16**:10, 1088-1099. [Abstract] [Full Text HTML] [Full Text PDF] [Full Text PDF with Links] [Supplemental material]
4. Tiziana Anelli , Leda Bergamelli , Eva Margittai , Alessandro Rimessi , Claudio Fagioli , Antonio Malgaroli , Paolo Pinton , Maddalena Ripamonti , Rosario Rizzuto , Roberto Sitia . 2012. Ero1# Regulates Ca2+ Fluxes at the Endoplasmic Reticulum–Mitochondria Interface (MAM). *Antioxidants & Redox Signaling* **16**:10, 1077-1087. [Abstract] [Full Text HTML] [Full Text PDF] [Full Text PDF with Links] [Supplemental material]
5. Milena Bertolotti , Roberto Sitia , Anna Rubartelli . 2012. On the Redox Control of B Lymphocyte Differentiation and Function. *Antioxidants & Redox Signaling* **16**:10, 1139-1149. [Abstract] [Full Text HTML] [Full Text PDF] [Full Text PDF with Links]
6. Gábor Bánhegyi , Éva Margittai , András Szarka , József Mandl , Miklós Csala . 2012. Crosstalk and Barriers Between the Electron Carriers of the Endoplasmic Reticulum. *Antioxidants & Redox Signaling* **16**:8, 772-780. [Abstract] [Full Text HTML] [Full Text PDF] [Full Text PDF with Links]
7. Taichi Kakihana , Kazuhiro Nagata , Roberto Sitia . 2012. Peroxides and Peroxidases in the Endoplasmic Reticulum: Integrating Redox Homeostasis and Oxidative Folding. *Antioxidants & Redox Signaling* **16**:8, 763-771. [Abstract] [Full Text HTML] [Full Text PDF] [Full Text PDF with Links]
8. Christine C. WinterbournBiological Chemistry of Reactive Oxygen Species . [CrossRef]
9. Philippe J. Nadeau, Annie Roy, Catherine Gervais-St-Amour, Marie-Ève Marcotte, Nathalie Dussault, Sonia Néron. 2012. Modulation of CD40-activated B lymphocytes by N-acetylcysteine involves decreased phosphorylation of STAT3. *Molecular Immunology* **49**:4, 582-592. [CrossRef]
10. Xi Wang, Likun Wang, Xi'e Wang, Fei Sun, Chih-chen Wang. 2011. Structural insights into the peroxidase activity and inactivation of human peroxiredoxin 4. *Biochemical Journal* . [CrossRef]
11. Jose Manuel Garcia-Manteiga, Silvia Mari, Markus Godejohann, Manfred Spraul, Claudia Napoli, Simone Cenci, Giovanna Musco, Roberto Sitia. 2011. Metabolomics of B to Plasma Cell Differentiation. *Journal of Proteome Research* 110729130128094. [CrossRef]
12. Ryszard Dworski, Wei Han, Timothy S. Blackwell, Aimee Hoskins, Michael L. Freeman. 2011. Vitamin E prevents NRF2 suppression by allergens in asthmatic alveolar macrophages in vivo. *Free Radical Biology and Medicine* **51**:2, 516-521. [CrossRef]
13. Emily M. Lynes, Thomas Simmen. 2011. Urban planning of the endoplasmic reticulum (ER): How diverse mechanisms segregate the many functions of the ER. *Biochimica et Biophysica Acta (BBA) - Molecular Cell Research* . [CrossRef]
14. Junichi Fujii, Satoshi Tsunoda. 2011. Redox regulation of fertilisation and the spermatogenic process. *Asian Journal of Andrology* **13**:3, 420-423. [CrossRef]
15. Matthias J Feige, Linda M Hendershot. 2011. Disulfide bonds in ER protein folding and homeostasis. *Current Opinion in Cell Biology* **23**:2, 167-175. [CrossRef]
16. Simone Cenci, Eelco van Anken, Roberto Sitia. 2011. Proteostenosis and plasma cell pathophysiology. *Current Opinion in Cell Biology* **23**:2, 216-222. [CrossRef]
17. Y. Ikeda, M. Nakano, H. Ihara, R. Ito, N. Taniguchi, J. Fujii. 2011. Different consequences of reactions with hydrogen peroxide and t-butyl hydroperoxide in the hyperoxidative inactivation of rat peroxiredoxin-4. *Journal of Biochemistry* **149**:4, 443-453. [CrossRef]
18. Éva Margittai, Roberto Sitia. 2011. Oxidative Protein Folding in the Secretory Pathway and Redox Signaling Across Compartments and Cells. *Traffic* **12**:1, 1-8. [CrossRef]